

## Optical properties of Al-doped a-Si:H films

This article has been downloaded from IOPscience. Please scroll down to see the full text article.

1999 J. Phys.: Condens. Matter 11 9619

(<http://iopscience.iop.org/0953-8984/11/48/319>)

View [the table of contents for this issue](#), or go to the [journal homepage](#) for more

Download details:

IP Address: 171.66.16.218

The article was downloaded on 15/05/2010 at 18:48

Please note that [terms and conditions apply](#).

## Optical properties of Al-doped a-Si:H films

Ahmed H El-Naggar and Assem M Bakry†

Physics Department, Faculty of Science, Ain-Shams University, Cairo, Egypt

Received 20 October 1998

**Abstract.** The effect of doping on a-Si:H film optical constants was studied. Evaporated films were doped with Al for making p-type material. The optical energy gap  $E_g$  decreased with increase in doping concentration. The Urbach parameter increased with doping. The refractive index decreased with increasing Al concentration showing a sharp rise in dispersion curve for p<sup>+</sup> samples. The absorption coefficient increased with doping and the absorption edge shifted to lower energies.

### 1. Introduction

Interest in hydrogenated amorphous silicon (a-Si:H) has been greatly increased by the suitability of a-Si:H for the fabrication of low-cost solar cells [1] and large area photodetectors [2]. The large absorption coefficient of a-Si in the visible spectral range has made this material very attractive for solar cell applications. A thickness of 1  $\mu\text{m}$  is sufficient to absorb most of the photons with energies above the a-Si:H band gap [3]. Moreover, the optical gap of a-Si:H can be varied over a wide range from about 1.0 eV to 2 eV by alloying with the appropriate impurity such as Ge [4], H [5] and C [6]. This provides considerable flexibility to optimize the spectral response of optoelectronic devices based on a-Si:H. The variation of the refractive index with doping and growth parameters also provides the means to tailor the refractive index to any desired value.

Doping in a-Si:H has been the subject of active research. Besides the desired shift of the Fermi level, doping in general affects the matrix network and produce bulk and surface effects [3, 5]. For producing p-type a-Si:H films, boron (B) has been mostly used as a dopant [3, 5, 7, 8]. The use of Al for doping a-Si:H has not been extensively studied [9].

In this work, we report results on the variation of the optical properties of a-Si:H films as a result of doping with aluminum.

### 2. Experimental details

The used films were prepared on Corning 7059 glass substrates at a temperature of 300 °C. Silicon was evaporated from an electron beam heated vitreous carbon crucible at a rate of approximately 3 Å per second to a thickness of about 5000 Å. The dopant material (Al) was thermally evaporated simultaneously with Si at different rates. The Si evaporation rate and thickness were controlled automatically by a quartz transducer. The thickness was also determined interferometrically [10].

† Corresponding author.

The base pressure of vacuum was  $10^{-7}$  mbar. During the entire evaporation process, atomic hydrogen was blown at the growing film from a radio frequency dissociation system. The resulting hydrogen pressure in the vacuum vessel was  $3 \times 10^{-5}$  mbar and the hydrogen flux through the dissociator was about  $16 \text{ ml N min}^{-1}$ . In this environment most dangling bonds in Si were saturated by hydrogen and the properties of amorphous films of pure Si are similar to those of a-Si:H prepared by silane decomposition [11].

Al concentrations were estimated from SIMS analysis where it was found to change from 2.4 to 8.3 at.% for Al. The hydrogen content in all the used films was kept fixed at  $C_H = 12 \text{ at.}\%$ .

The transmission ( $T$ ) and reflection ( $R$ ) spectra were carried out between 200 and 3000 nm in steps of 2 nm using a computer-aided double-beam spectrophotometer (Shimadzu 3101 PC UV-VIS-NIR). The relative uncertainty in the transmittance and reflectance given by manufacturer is 0.2%. Transmittance scans were performed using a glass substrate in the reference compartment of the same kind as the one used for the film deposition. The transmittance and reflectance were measured at the same incidence angle of 5 degrees.

### 3. Methods of calculation

The transmission and reflection spectra were measured in the range 200–3000 nm. The absolute values of measured transmittance and reflectance after correcting for the absorbance and reflectance of the substrate are calculated as follows [12–14]:

$$I_{ft} = I_0 T (1 - R_g) (1 - A_g)$$

where  $I_{ft}$  is the intensity of light passing through the film–glass system,  $R_g$  the reflectance of glass and  $A_g$  the glass absorbance.

$$I_g = I_0 (1 - R_g)^2 (1 - A_g)$$

where  $I_g$  is the intensity of light passing through the reference glass.

Since the substrate is non-absorbing, i.e.  $A_g = 0$ , then

$$\frac{I_{ft}}{I_g} = \frac{T}{(1 - R_g)} \quad T = \left( \frac{I_{ft}}{I_g} \right) (1 - R_g). \quad (1)$$

Considering

$$R = \frac{I_{fr}}{I_m} R_m [1 + (1 - R_g)^2 (1 - A_g)^2] - T^2 R_g$$

where  $I_m$  is the intensity of light reflected from the reference mirror,  $I_{fr}$  the intensity of light reflected from the sample reaching the detector and  $R_m$  the mirror reflectance.

Considering  $A_g = 0$ ,

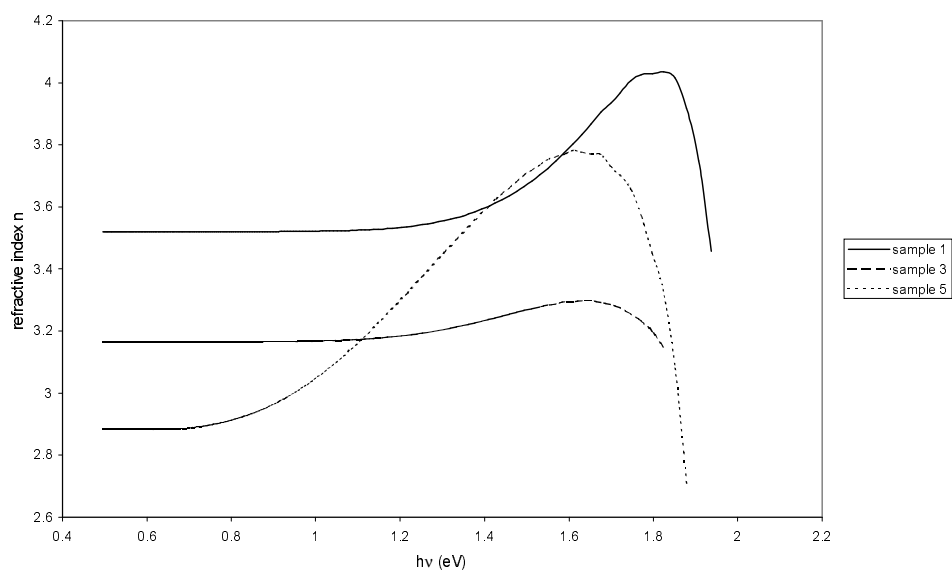
$$R = \left( \frac{I_{fr}}{I_m} \right) R_m [1 + (1 - R_g)^2] - T^2 R_g. \quad (2)$$

In order to calculate the refractive index  $n$  and extinction coefficient  $k$ , we used the method suggested by Manificier *et al* [15] and modified by Swanepoel [16]. According to Swanepoel [17], in the case of inhomogenities in thin films there is a considerable shrinking of the interference fringes of the optical transmission spectrum. No such shrinking was found in the obtained spectrum, indicating uniformity of the films.

The spectral envelopes of the transmittance,  $T_{max}(\lambda)$  and  $T_{min}(\lambda)$ , which are assumed to be continuous functions of the wavelength, were computed using a polynomial interpolation between extrema.

**Table 1.** Measured values of Al content, refractive index  $n$  and Urbach parameter  $E_0$  for the used samples.

Sample	Al (at.%)	$n$ ( $h\nu = 0.5$ eV)	$E_0$ (meV)
1	0	3.52	73
2	2.4	3.17	104
3	3.6	3.16	120
4	5.6	3.0	134
5	8.3	2.88	177

**Figure 1.** The dispersion of the refractive index  $n(\lambda)$  for samples with different doping concentrations.

#### 4. Results and discussion

A list of the used samples with different doping concentrations is given in table 1. The use of Al with concentrations less than 2 at.% has been tested. No significant change in the optical properties was observed, in agreement with previous attempts [9].

The refractive index  $n$  is plotted as a function of the photon energy  $h\nu$  in figure 1 for the undoped film (sample 1) and two of the doped samples. As shown in the figure, the refractive index in the measured energy range between 0.5 and 2 eV exhibits a strong dispersion due to the onset of interband transitions and reaches values as high as  $n = 4.1$  at 1.8 eV for the intrinsic film. Similar dispersion curves were reported by Cody *et al* [18] between 1 and 4 eV and Klazes *et al* [19] between 0.6 and 3 eV.

Values of  $n$  over the entire measured spectrum decreased with increase in doping. The same behaviour was reported by Brodsky *et al* [20] when using  $B_2H_6$  for doping. It has been shown by Dusane *et al* [8] that in  $B_2H_6$  doped a-Si:H, the defect density increased by almost three orders of magnitude. This was due to an increase in bond angle deviations with increasing dopant concentrations. The increase in bond angle deviations causes internal strain in the amorphous network. The increase in the internal strain in the present case is the probable cause for decrease of refractive index with doping by Al. The heavily doped

film, sample 5, showed a more sharply rising dispersion, in agreement with previous results [20].

The change of the real part of the dielectric constant  $\varepsilon_1$  with doping is illustrated in figure 2. Similar curves were shown by others in the energy range 0.5 to 4 eV [3, 21].

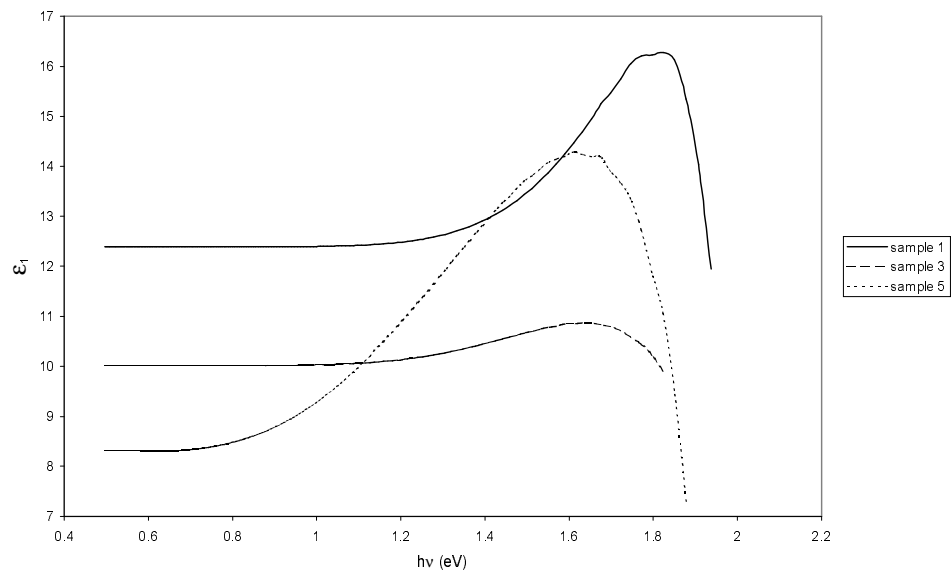


**Figure 2.** The effect of doping on the real part of the dielectric constant  $\varepsilon_1$ .

In figure 3, the refractive index  $n$  is plotted as a function of Al concentration for  $h\nu = 0.5$  eV. The incorporation of Al decreases the refractive index for doping concentrations starting from 2.4 up to 8.3 at.%. Brodsky and Leary [20], using 1%  $B_2H_6$ , agree with our results for  $n$ . Nitta *et al* [22] using the same dopant and concentration as Brodsky reported a change in the optical properties with no details about this change concerning the refractive index. However, Schmal *et al* [23], when using triethylboron  $(C_2H_5)_3B$ , did not realize any changes in the refractive index. The opposite behaviour was observed by Hadjadj *et al* [7] for doping concentrations above  $10^{-3}$   $B_2H_6$ , where the refractive index increased strongly. For doping levels less than  $10^{-3}$ ,  $n$  values were not affected.

Considering the present results and those previously reported, the change of  $n$  with doping is dependent on the preparation conditions as well as the kind of dopant used.

The absorption curves of intrinsic and heavily doped films are shown in figure 4. The curves exhibit the characteristic behaviour of a-Si:H material [3, 5, 21]; the existence of an exponential absorption tail (Urbach tail) and a defect related subgap absorption due to deep defect levels (dangling bonds). As seen in figure 4, the absorption coefficient  $\alpha$  shifts to higher values with doping. Similar results were shown by others [7, 20, 24]. The enhancement of the absorption at low energies is attributed to the increase on the density of defects induced by doping, i.e., increase in structural disorder.

The changes induced by Al doping in the imaginary part of the dielectric constant  $\varepsilon_2$  are shown in figure 5. The amplitude of  $\varepsilon_2$  is higher in doped film and the position of the peak is shifted to lower energies by  $\approx 0.14$  eV.

The Urbach tail was found to be related directly to a similar exponential tail for the density of states of either one of the two band edges [3, 25, 26]. The width of the Urbach tail is an

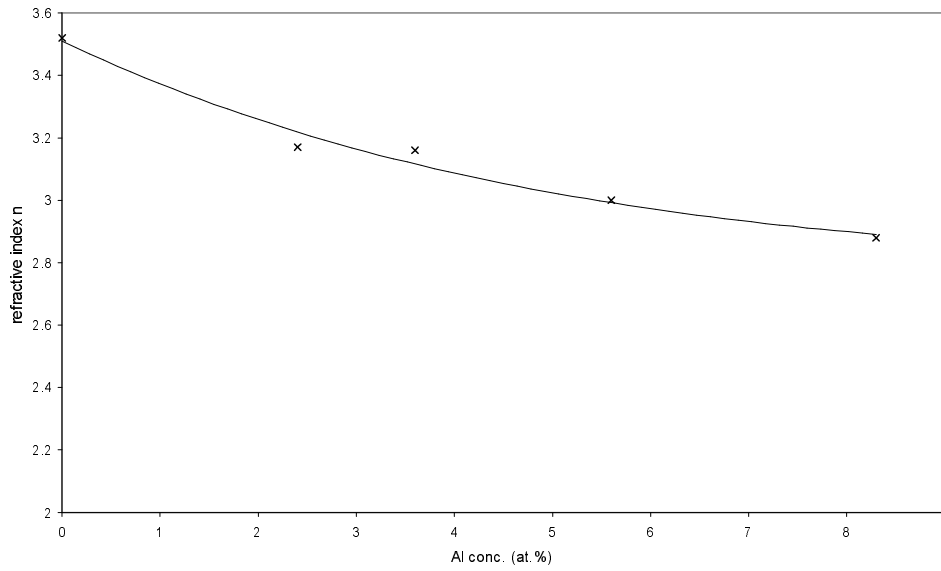


**Figure 3.** Modifications of the refractive index, at  $h\nu = 0.5$  eV, with Al doping.

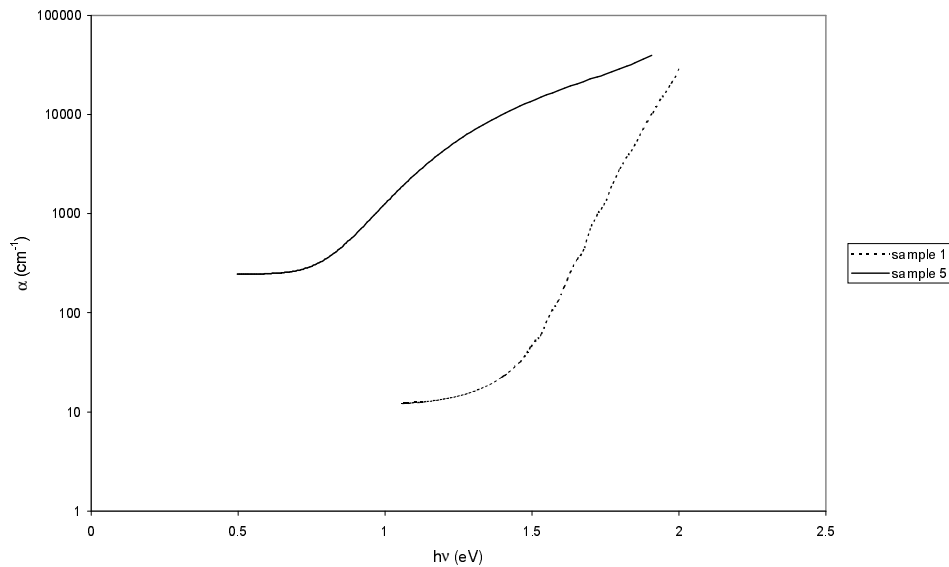


**Figure 4.** The shift of the absorption coefficient due to doping effects.

indicator of disorder in the material. The following relation was used to calculate the slope of the Urbach tail [3]:

$$\alpha(h\nu) = \alpha_0 \exp\left(\frac{h\nu - E^*}{E_0}\right)$$

where  $E^*$  is the onset of the exponential tail and  $E_0$  is the parameter defining the slope (width) of the tail. The values of  $E_0$  for the used films are listed in table 1. The increase of  $E_0$  with

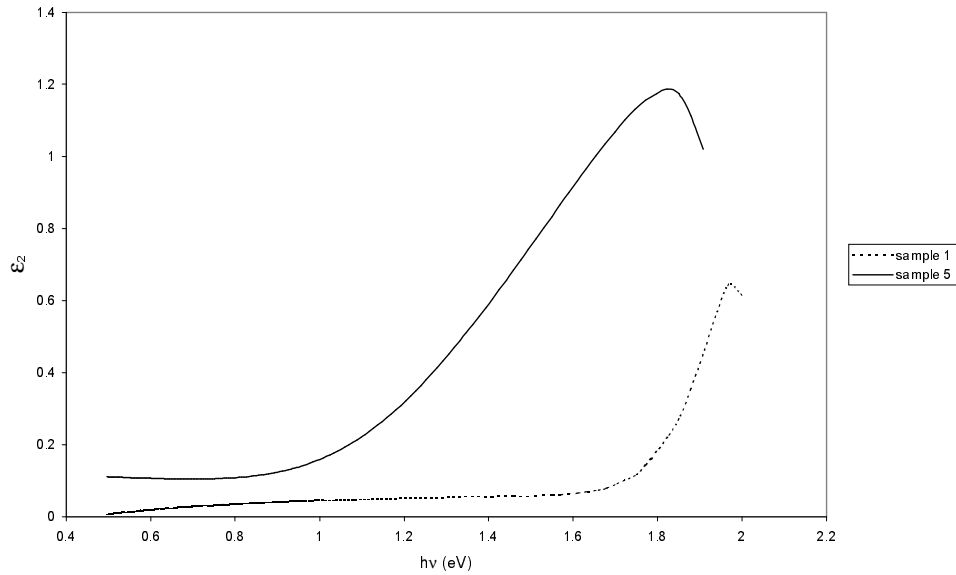


**Figure 5.** The change in the imaginary part of the dielectric constant with doping.

**Table 2.** Values of  $E_g$  (in eV) calculated using different plots.

Sample	$(\alpha h\nu)^{1/2}$	$(\alpha/h\nu)^{1/2}$	$(\alpha h\nu)^{1/3}$
1	1.77	1.75	1.66
2	1.64	1.17	1.12
3	1.58	1.52	1.33
4	1.53	1.44	1.37
5	1.31	1.07	1.03

doping indicates an increase in disorder in the a-Si:H material. The value of  $E_0$  for the intrinsic sample agrees with previously published values [27] using  $H$  concentration of  $\approx 13\%$ , which is close to the value used in this study.

To define the optical gap,  $E_g$ , Tauc *et al* [28] proposed the expression

$$(\alpha h\nu) = C_0(h\nu - E_g)^2.$$

$E_g$  was then calculated by a linear extrapolation of the  $(\alpha h\nu)^{1/2}-h\nu$  plot to the energy axis. The physical basis of the Tauc expression are the assumptions of parabolic energy bands, an energy-independent momentum matrix element and a relaxation of momentum conservation. More recently, Cody [21] has suggested an alternative expression,

$$(\alpha/h\nu) = B_0(h\nu - E_g)^2.$$

This expression was obtained assuming parabolic bands and an energy-independent dipole matrix element. Cody showed that his expression defines an energy gap that is independent of the energy range over which  $\alpha$  is determined and hence independent of the thickness of the film. Klazes *et al* [19], assuming a linear distribution of energy states near the bandgap and equal matrix elements for interband transitions, reached the following expression for  $E_g$  determination:

$$(\alpha h\nu) = c(h\nu - E_g)^3.$$

The above expression was assumed to produce a linear fit over a wider range in  $h\nu$ .

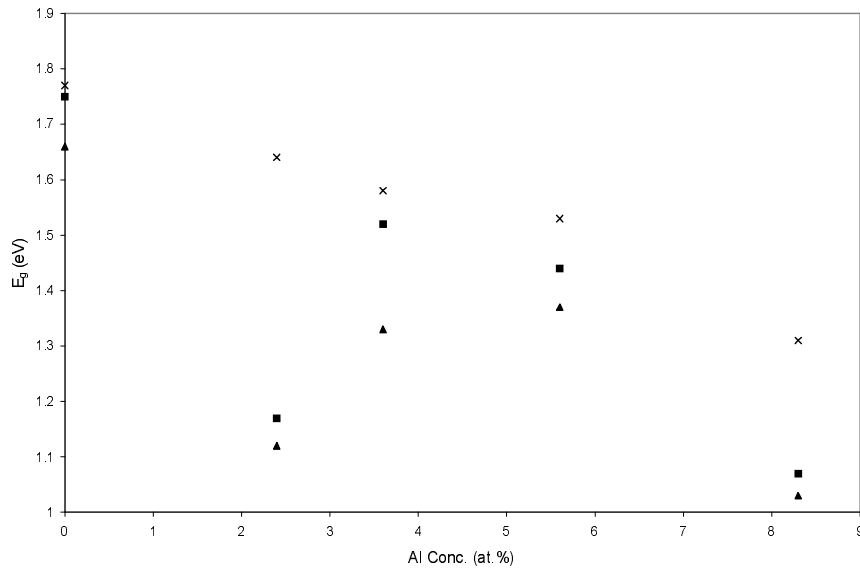


Figure 6. Comparison between different plots used for determination of  $E_g$ .

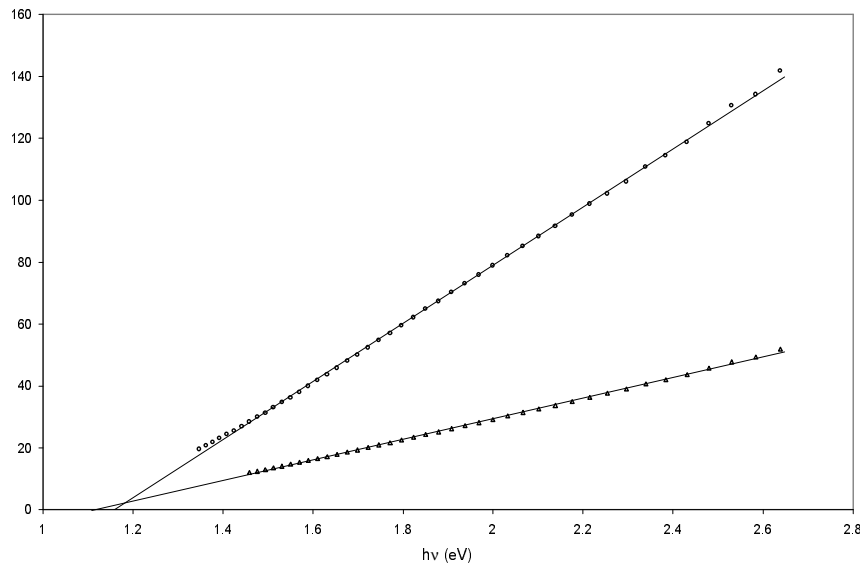


Figure 7. The  $(\alpha/h\nu)^{1/2}$  and  $(\alpha/h\nu)^{1/3}$  plots for sample 2.

The above three expressions for  $E_g$  were implemented in this study for comparison. The values of  $E_g$  using different expressions are listed in table 2. Figure 6 illustrates the change in  $E_g$  with doping with respect to different approximations made for  $\alpha(E)$ . For the Tauc plot,  $(\alpha h\nu)^{1/2}$ , there is a continuous decrease in  $E_g$  with doping, in agreement with Talukder *et al* [9] using Al for doping. The decrease in  $E_g$  is attributed to the increase of disorder of the material caused by doping. This increase leads to a redistribution of states, from band to tail, thus allowing for a greater number of possible band to tail and tail to tail transitions [26]. As a

result, both a decrease in the optical gap and a broadening of the absorption tail (Urbach tail) occur.

As for the  $(\alpha/h\nu)^{1/2}-h\nu$  and  $(\alpha h\nu)^{1/3}-h\nu$  plots, better linearity over a wider range of  $h\nu$  was achieved for some films. This is illustrated in figure 7. However, values of  $E_g$  for some of the samples were much less than those obtained using Tauc's expression, which are in agreement with published values. This might cause some ambiguity in defining  $E_g$  using those two plots. As a result, we suggest using Tauc's definition for  $E_g$  with the consideration of a suitable range for  $\alpha$ . The same conclusion was reached by others [22, 29].

## 5. Conclusions

The optical properties of Al-doped p-type a-Si:H samples were studied and the following conclusions were drawn.

- (1) The refractive index  $n$  decreased from 3.52 at  $h\nu = 0.5$  eV for intrinsic samples to  $n = 2.88$  for  $p^+$  samples, thus making it possible to tailor the refractive index to a certain value. As the doping concentration increases, the dispersion rises more sharply.
- (2) The absorption coefficient increased with doping and the absorption edge shifted to lower energy values.
- (3) The optical band gap ( $E_g$ ) was calculated using three different expressions, namely  $(\alpha h\nu)^{1/2}$ ,  $(\alpha/h\nu)^{1/2}$  and  $(\alpha h\nu)^{1/3}$ . The square-root formula of Tauc was better for defining the optical gap of doped a-Si:H films.
- (4) Values of the Urbach parameter  $E_0$  increased with doping from 73 meV for intrinsic to 177 meV for concentrations of 8.3 at.% Al. This indicates an increase in the disorder of the material.
- (5) The optical gap decreased with increase in doping. This was attributed to the increase of defects induced by doping.
- (6) Using Al as a dopant for a-Si:H material has almost the same effect on the optical properties as B.

## Acknowledgment

The authors would like to thank Professor Mahmoud El-Nahass for his great help in getting this work done.

## References

- [1] Carlson D E and Wronski C R 1976 *Appl. Phys. Lett.* **28** 671
- [2] Imamura Y, Ataka S, Takasaki Y, Kusano C, Hirai T and Maruyama E 1979 *Appl. Phys. Lett.* **35** 349
- [3] Stutzmann M 1994 *Handbook on Semiconductors* vol 3A, ed S Mahajan (Amsterdam: North-Holland) p 657
- [4] Paul W, Paul D K, Von Roedern B, Blake J and Oguz S 1981 *Phys. Rev. Lett.* **49** 1016
- [5] Ley L 1984 *The Physics of Hydrogenated Amorphous Silicon II* ed J D Joannopoulos and G Lucovsky (Berlin: Springer) p 61
- [6] Basu N, Ganguly G, Ray S and Barua A K 1989 *Japan. J. Appl. Phys.* **28** 1776
- [7] Hadjadj A, St'ahel P, Cabarrocas P, Paret V, Bounouth Y and Martin J C 1998 *J. Appl. Phys.* **83** 830
- [8] Dusane R O, Dusane S R, Bhide V G and Kshirsagar S T 1991 *J. Non-Cryst. Solids* **137/138** 115
- [9] Talukder G, Cowan J A, Brodie D E and Leslie J D 1984 *Can. J. Phys.* **62** 848
- [10] Tolansky S 1970 *Multiple-Beam Interference. Microscopy of Metals* (London: Academic) p 55
- [11] Gosh A K, McMahan T, Rock E and Wiesmann H 1979 *J. Appl. Phys.* **50** 3407
- [12] Agier L A and Shklyareveski I N 1978 *J. Prekel. Spekt.* **76** 380
- [13] Shklyareveski I N, Kornveeva T I and Zozula K N 1969 *Opt. Spectrosc.* **27** 174

- [14] Arndt D P 1984 *Appl. Opt.* **23** 3571
- [15] Manificier J C, Gasiot J and Fillard J P 1976 *J. Phys. E: Sci. Instrum.* **9** 1002
- [16] Swanepoel R 1983 *J. Phys. E: Sci. Instrum.* **16** 1214
- [17] Swanepoel R 1984 *J. Phys. E: Sci. Instrum.* **17** 896
- [18] Cody G D, Abeles B, Wronski C R and Brooks B 1980 *J. Non-Cryst. Solids* **35/36** 463
- [19] Klazes R H, Van Den Broek M H, Bezemer J and Radelaar S 1982 *Phil. Mag.* **B 45** 377
- [20] Brodsky M H and Leary P A 1980 *J. Non-Cryst. Solids* **35/36** 487
- [21] Cody G D 1984 *Semiconductors and Semimetals* vol 21, ed J I Pankove (New York: Academic) p 11
- [22] Nitta S, Itoh S, Tanaka M, Endo T and Hatano A 1982 *Sol. Energy Mater.* **8** 249
- [23] Schmal J, Kirsch R, Albert M, Stahr F and Bindemann R 1993 *J. Non-Cryst. Solids* **164-166** 415
- [24] Freeman E C and Paul W 1979 *Phys. Rev. B* **20** 716
- [25] Cody G D 1992 *J. Non-Cryst. Solids* **141** 3
- [26] O'Leary S K, Zukotynski S and Perz J M 1997 *J. Non Cryst. Solids* **210** 249
- [27] Cody G D, Tiedje T, Abeles B, Brooks B and Goldstein Y 1981 *Phys. Rev. Lett.* **47** 1480
- [28] Tauc J, Grigorovici R and Vancu A 1966 *Phys. Status Solidi* **15** 627
- [29] Kruzelecky R V, Ukah C, Racansky D, Zukotynski S and Perz J M 1988 *J. Non-Cryst. Solids* **103** 234